Mapping Light-Dependent Structural Changes in the Cytoplasmic Loop Connecting Helices C and D in Rhodopsin: A Site-Directed Spin Labeling Study†

Zohreh Toossi Farahbakhsh,‡ Kevin D. Ridge,§,|| H. Gobind Khorana,*,|| and Wayne L. Hubbell*,‡

Jules Stein Eye Institute and the Department of Chemistry and Biochemistry, University of California, Los Angeles, California 90095-7008, and Departments of Biology and Chemistry, Massachusetts Institute of Technology, 77 Massachusetts Avenue, Cambridge, Massachusetts 02139

Received February 17, 1995; Revised Manuscript Received April 17, 1995⊗

ABSTRACT: All 20 single cysteine substitution mutants in the sequence Y136−M155 of bovine rhodopsin have been prepared and modified with a sulfhydryl-specific nitroxide reagent. This sequence contains the C−D interhelical loop, a transducin interaction site. The accessibilities of the attached nitroxides to collisions with paramagnetic probes in solution were determined, and the electron paramagnetic resonance spectra were analyzed, both in the dark and after photoexcitation. Accessibility data show that the rhodopsin polypeptide crosses an aqueous/hydrophobic boundary near V138 and H152. The nitroxide mobilities inferred from the spectra are consistent with a model where the C helix extends to at least residue C140, with much of the helix surface in contact with protein rather than lipid near the cytoplasmic surface of the membrane. Upon photoexcitation, electron paramagnetic resonance spectral changes are observed at sites on the putative C helix surface that are in contact with the protein and at specific sites in the C−D interhelical loop. A simple interpretation of these results is that photoexcitation involves a rigid body movement of the C helix relative to the others in the helix bundle.

Rhodopsin is the membrane-bound photoreceptor protein of the vertebrate rod cell. Upon the isomerization of the 11-*cis*-retinal chromophore by light, rhodopsin undergoes a conformational change of unknown nature at the cytoplasmic surface that leads to activation of transducin, the visual G protein (Konig et al., 1989). The protein has been sequenced at both the cDNA and protein levels and contains 348 amino acids. A wealth of biochemical and biophysical data indicate that rhodopsin contains seven transmembrane α-helices in a motif similar to that of bacteriorhodopsin [see Ovchinnikov (1982) and Khorana (1992) for reviews]. Hydropathy considerations suggest an intersection of the membrane/solution boundaries with the helices approximately as shown in the secondary structural model of Figure 1. Recently, an electron density map in projection at 9 Å resolution has been obtained from two-dimensional crystals of bovine rhodopsin, sufficient to resolve some of the helices (Schertler et al., 1993). On the basis of sequence comparisons of 204 members of the G-protein-coupled receptor family, Baldwin (1993) has proposed an approximate packing arrangement of the helices consistent with the projected electron density.

Thus the general motif of the rhodopsin structure seems clear. However, the structural organization is not known in detail, and many questions remain regarding structure and functional relationships. Of particular interest is the mechanism by which the isomerization of retinal, buried deep in the molecule, results in distal changes in structure at the cytoplasmic surface. An attractive model for the propagation of structural changes through the molecule is rigid body movements of the α-helical segments, a mechanism with precedent in conformational changes of water-soluble proteins (Chothia & Lesk, 1985; McPhalen et al., 1992).

The method of site-directed spin labeling has proven to be a useful approach for the investigation of membrane protein structure and dynamics [see Hubbell and Altenbach (1994) for a recent review]. The general experimental approach has been to introduce single reactive cysteine residues in the protein to provide attachment points for nitroxide spin labels. Analysis of the EPR[1] spectral line shapes and accessibilities of the attached nitroxides to collision with paramagnetic reagents in solution has been previously used to (1) determine topology in membrane proteins (Altenbach et al., 1989; Greenhalgh et al., 1991), (2) locate helical regions and their orientation (Altenbach et al., 1990), (3) determine the depth of immersion of residues on the outer surface of a transmembrane helix (Altenbach et al., 1994), and (4) follow protein conformational changes (Resek et al., 1993; Farahbakhsh et al., 1993; Shin et al., 1993; Steinhoff et al., 1994).

In the experiments reported here, spin-labeled single cysteines mutants of rhodopsin were prepared at 20 consecutive positions throughout the sequence Y136−M155, which contains the putative C−D interhelical loop (Figure 1). The results obtained extend earlier studies of a light-induced conformation change detected by a spin label at C140 in

† This is paper 14 in the series "Structure and Function of Rhodopsin". Research reported here was supported by NIH Grants EY05216 (W.L.H.) and GM28289 (H.G.K.), by the Research to Prevent Blindness Foundation (W.L.H.), and by the Jules Stein Professorship Endowment (W.L.H.). K.D.R. was the recipient of National Institutes of Health Research Service Award 5F32 EY06269.

* To whom correspondence should be addressed.

‡ Jules Stein Eye Institute and UCLA.

§ Present Address: Center for Advanced Research in Biotechnology (CARB), 9600 Gudelsky Dr., Rockville, MD 20850.

|| Massachusetts Institute of Technology.

⊗ Abstract published in *Advance ACS Abstracts,* June 15, 1995.

[1] Abbreviations: EPR, electron paramagnetic resonance; DM, *n*-dodecyl-β-D-maltoside; MI, metarhodopsin I; MII, metarhodopsin II; NiEDDA, nickle (II) ethylenediaminediacetate; NiAA, nickle(II) acetonylacetonate.

0006-2960/95/0434-8812$09.00/0

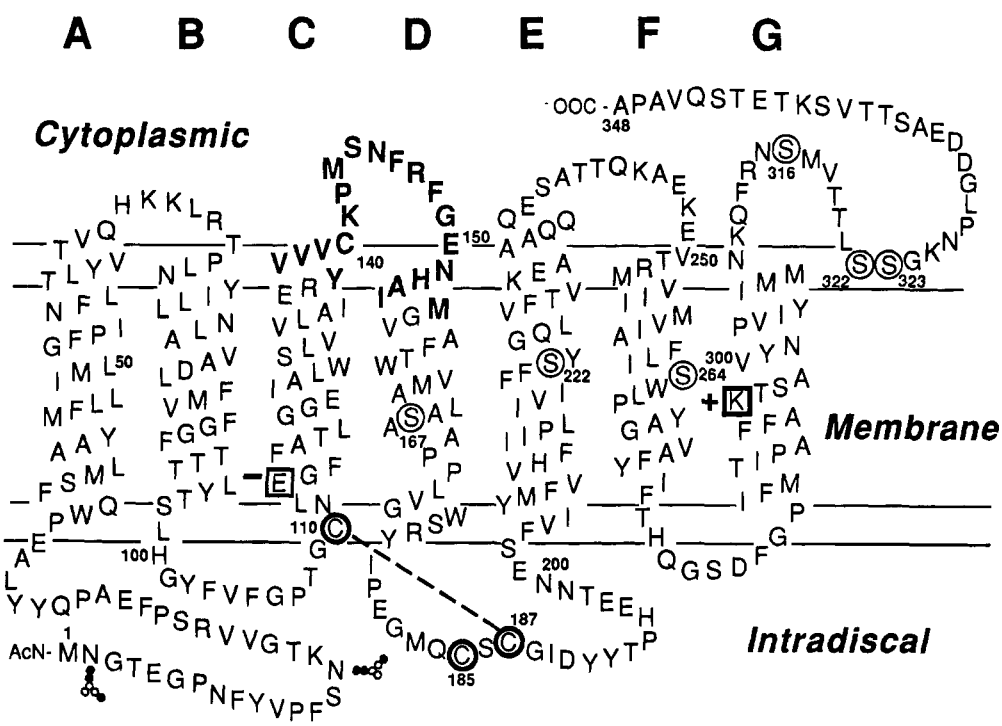

FIGURE 1: Secondary structural model of rhodopsin. The sites included in this study, 136−155, are highlighted in bold type. The positions of the native cysteine residues replaced by serine are circled. The attachment site of retinal, K296, and the counterion to the protonated Schiff base, E113, are boxed. The double horizontal lines define the approximate domain of the polar head-group regions of the phospholipid bilayer.

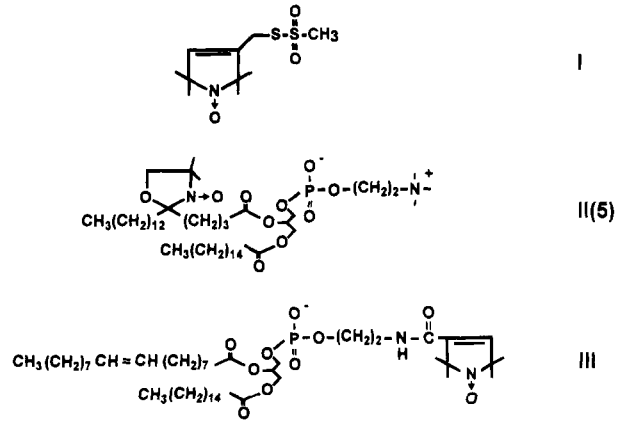

FIGURE 2: Structures of the spin labels.

this region (Resek et al., 1993; Farahbakhsh et al., 1993) and provide information on the probable structure in this transducin-binding region of the receptor.

EXPERIMENTAL PROCEDURES

Materials. Restriction endonucleases were obtained from Boehringer Mannheim Biochemicals (Indianapolis, IN) and New England Biolabs (Beverly, MA). Sequenase (version 2.0) was from United States Biochemical (Cleveland, OH), and DM was purchased from Anatrace (Maumee, OH). 11-*cis*-Retinal was a gift from P. Sorter (Hoffman LaRoche) and R. Crouch (Medical University of South Carolina). Deoxyadenosine 5′-α-[^{35}S]thiotriphosphate (500 Ci/mmol) was from Dupont−New England Nuclear (Boston, MA).

The sulfhydryl-specific spin label (1-oxyl-2,2,5,5-tetramethylpyrroline-3-methyl)methanethiosulfonate I (Figure 2) was a gift of Kálmán Hideg (University of Pecs, Pecs, Hungary) and is commercially available from Reanal (Budapest, Hungary). Spin-labeled phospholipids II(n) with a nitroxide at various positions along the 2-acyl chain were purchased from Avanti Polar Lipids (Birmingham, AL). In referring to these lipids, the index n designates the number of the carbon atom bearing the nitroxide, with the carbonyl carbon as 1. The structure is illustrated by II(5) in Figure 2. The phospholipid III (Figure 2) was a gift from Christian Altenbach (University of California, Los Angeles).

Construction of Mutant Opsin Genes. The base Cys-mutant gene contained Cys>Ser replacement at the native cysteine positions 140, 167, 222, 264, 316, 322, and 323 (Karnik et al., 1988; see Figure 1). The construction of mutants carrying Cys replacements at amino acids 136−150 in the base Cys-mutant gene is described in the preceding paper (Ridge et al., 1995a). Mutants carrying cysteine replacements at amino acids 151−155 were constructed using the same strategy, and all mutations were confirmed by dideoxynucleotide sequencing of CsCl purified DNA (Sanger et al., 1977).

Expression, Purification, and Characterization of Mutant Rhodopsin. The methods used were similar to those reported in the preceding paper (Ridge et al., 1995a). Briefly, the opsin genes were transiently expressed in COS-1 cells as previously described (Oprian et al., 1987; Karnik et al., 1993). At ≈60 h posttransfection, the cells were harvested and washed with 10 mM NaH_2PO_4, pH 7.0, containing 150 mM NaCl, and the rhodopsin chromophore was regenerated by the addition of 5 μM 11-*cis*-retinal to the cell suspension for 3 h at 4 °C in the dark. The cells were solubilized in 1% DM and the mutants purified by immunoaffinity chromatography on 1D4-Sepharose (Oprian et al., 1987). The resin was washed five times with 20 column volumes of (i) 20 mM Tris-HCl, pH 8.0, containing 2 mM ATP, 2 mM $MgCl_2$, 1 M NaCl, and 0.1% DM, followed by (ii) 2 mM NaH_2PO_4, pH 6.0, containing 0.1% DM. The bound rhodopsin was eluted with 35 μM c′ 1−18 peptide in 2 mM

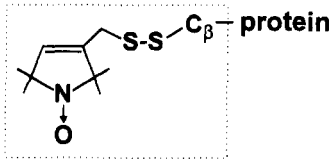

side-chain R1

FIGURE 3: Structure of the nitroxide side chain R1.

NaH_2PO_4, pH 6.0, containing 0.1% DM. Spectroscopic measurements of the proteins were performed with a Perkin-Elmer $\lambda 7$ UV/visible spectrophotometer. Wild-type and mutant rhodopsins purified in this manner typically had absorbance ratios (A_{280}/A_{500}) of 1.6−1.8.

Spin Labeling and EPR Spectroscopy of Rhodopsin Mutants. The rhodopsin mutants were derivatized with 500 μM spin label reagent I in the dark while bound to 1D4 Sepharose (Resek et al., 1993). Typically, the resin was washed three times with 20 column volumes of 50 mM Tris-HCl, pH 8.0, containing 150 mM NaCl, 2 mM EDTA, and 0.02% DM before addition of the spin label. After 6 h at 20 °C, the resin was extensively washed with 2 mM Na_2PO_4, pH 6.0, containing 0.1% DM to remove unreacted spin label, and the bound rhodopsin was eluted as described above.

Reaction of the spin label I with cysteine produces a new side chain containing a disulfide-linked nitroxide, which will be referred to as R1 (Figure 3). The various spin-labeled substitution mutants are designated by giving the original residue, the amino acid number, and the new residue. For example, a mutant first substituted with cysteine for the native valine at position 138 and then modified with I is designated V138R1.

Solutions of spin-labeled rhodopsin mutants (≈50 μg in 200 μL) were concentrated to a final volume of 10−20 μL using filtration units (Millipore Ultrafree-MC, 10 000 MW cutoff). This step also results in a concentration of DM to as high as ≈2% (w/v). This is in fact advantageous, since it has previously been shown that rhodopsin thermal stability increases with increasing concentration of DM up to at least 200 mM (Knudsen & Hubbell, 1978). Due to the small final volume in the filtration unit and losses on the filter, it was not possible to reproducibly obtain equal concentrations of protein and detergent in the different samples. This is mentioned, since differences in detergent concentration in the samples may be the origin for some variability in rhodopsin properties (see Results).

Samples of ≈2 μL were loaded in quartz capillaries and the EPR spectra recorded under field-frequency lock with a Varian E-109 spectrometer operating at X band and fitted with a loop-gap resonator (Hubbell et al., 1987). The microwave power was 2 mW incident, and the modulation amplitude was constant for all samples at 3 G. Signal averaged spectra (16 scans) were obtained with a 100 G sweep at 30 s/scan using a Nicolet 1280 computer. Spectra were recorded both in the dark and after 1 min of photobleaching with a fiber optic illuminator (Cole Parmer, Chicago, IL) equipped with a long wavelength pass filter (Melles-Griot, $\lambda \geq 500$ nm) and an infrared filter. Previous studies indicated that the majority of the pigment was in the MII state under the conditions described (Resek et al., 1993).

To obtain difference spectra due to photobleaching, the light and dark spectra were doubly integrated and normalized to a constant spin content. This was necessary to correct for variation in signal intensity resulting from removal and replacement of the sample during the photobleaching procedure. Errors in this integration would give difference spectra even in cases where no line shape changes occured. However, this situation is easily recognized, since the difference spectrum has a line shape identical to the starting spectra. In these cases, the spectra were scaled to give a null difference. Horizontal alignment of the spectra for subtraction was acheived through the use of a Varian field-frequency lock accessory. Small errors in alignment would also lead to a difference spectrum even in samples where no light-dependent changes occurred. This error can be recognized, since the difference spectrum would be the second derivative of the initial spectral line shape. Each difference spectrum was examined for the above errors. Occasionally, a small difference spectrum could be attributed to integration errors, but none could be traced to errors in alignment.

Power saturation measurements for the spin labels attached to rhodopsin were carried out as previously described (Resek et al., 1993) in the presence of O_2 in equilibrium with air and 20 mM NiEDDA and analyzed in terms of the parameter $\Delta P_{1/2}$ (Altenbach et al., 1989).

RESULTS

Characterization of the Spin-Labeled Mutants. The base Cys-mutant contains the disulfide-bonded C110 and C187 as well as C185, the latter of which is unreactive to sulfhydryl reagents in the folded protein. Thus, there was no detectable EPR spectrum after incubation of the base Cys-mutant with I and subsequent removal of excess label (data not shown).

All of the single cysteine replacement mutants reacted with spin label I in the dark (ground state) to give the EPR spectra shown in Figure 4 (heavy trace, left hand panel). Quantitative determination of the extent of reaction with each mutant in the 136−155 series was not carried out due to the small amounts of samples. However, previous studies showed that the reaction of I with several single cysteine mutants in the cytoplasmic domain of rhodopsin in DM, including C140, was essentially complete under the conditions used here (Resek et al., 1993). Incomplete reaction of a cysteine would only effect the magnitude of the EPR signal, and none of the results to follow are based on absolute signal amplitude. Figure 5 shows representative UV/visible spectra for V138R1 and K141R1. The spectra for all of the spin-labeled mutants were essentially identical and showed an absorption maximum at 500 nm characteristic of the native chromophore. As will be discussed below, the spin labels in V138R1 and K141R1 are at buried and exposed sites, respectively. It is significant that no perturbation in spectral properties is produced by introduction of the side chain R1 at a buried site.

Topography of the Sequence 136−155. Information on the topographical location of nitroxide side chains relative to the membrane−solution interface can be obtained by determining the collision rate of the nitroxide with paramagnetic reagents of both nonpolar (R_{np}) and polar (R_p) character. For this purpose, it is convenient to define the function $\Phi = \ln [\Delta P_{1/2}(R_{np})/\Delta P_{1/2}(R_p)]$, where $\Delta P_{1/2}$ is an experimental quantity proportional to the collision rate of the nitroxide with the paramagnetic reagent (Altenbach et

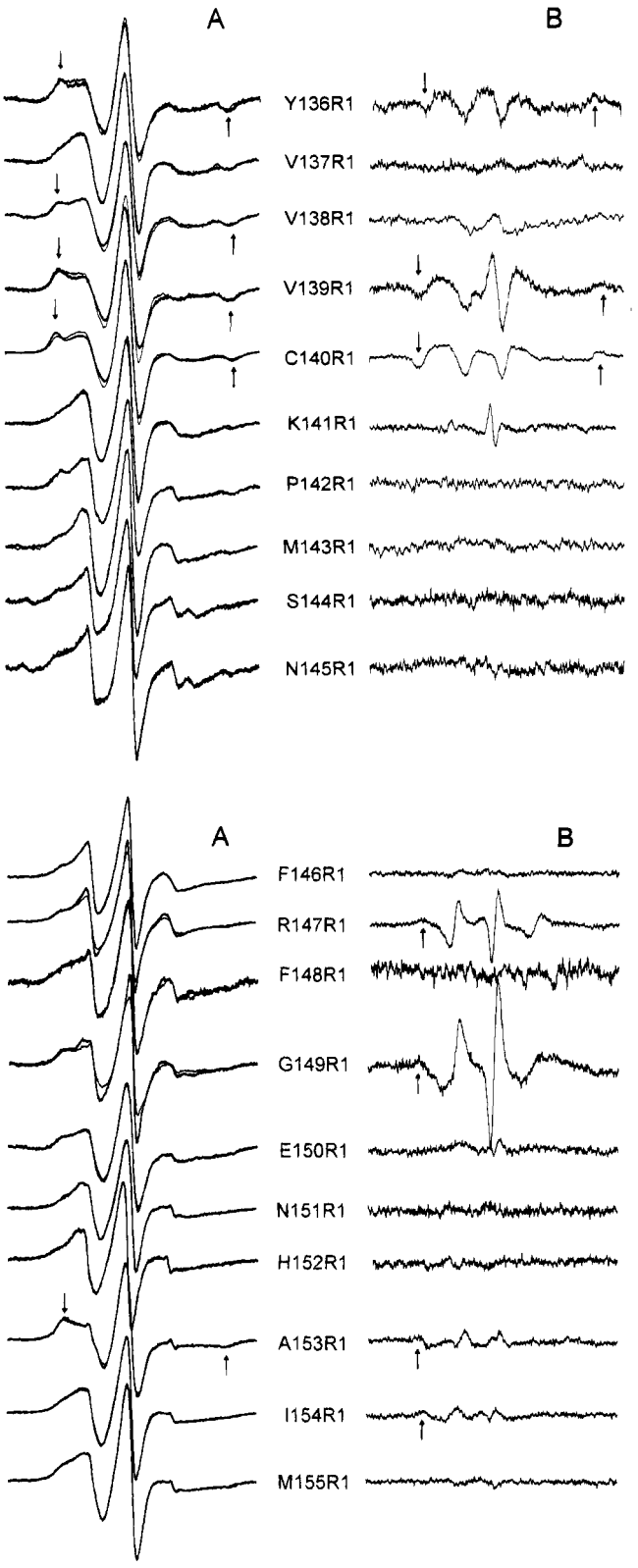

FIGURE 4: EPR spectra and EPR difference spectra. (A) First-derivative EPR spectra of the indicated rhodopsin mutant in the dark (heavy trace) and after photoactivation (light trace). Spectra are scaled for convenience of presentation. The arrows indicate positions of well-resolved outer hyperfine extrema in some of the spectra. (B) EPR difference spectra, (photoactivated-dark) states. The difference spectra are presented on the same scale, and the amplitudes reflect the correct relative changes observed for the same number of spins for each mutant. The upward and downward arrows indicate increases and decreases in intensity of the outer hyperfine extrema, respectively.

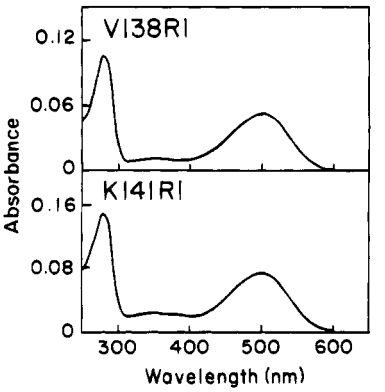

FIGURE 5: UV−visible spectra for two representative spin-labeled cysteine mutants (V138R1 and K141R1). The spectra are similar for all spin-labeled mutants and have spectral ratios (A_{280}/A_{500}) between 1.6 and 1.8.

al., 1994). The value of $\Delta P_{1/2}$ for any reagent depends on the protein structure around the nitroxide and the diffusion coefficient and local concentration of reagent. However, Φ itself is not strongly dependent on protein structure, since steric factors involved in the collision event approximately cancel in forming the ratio of $\Delta P_{1/2}$ values for two different reagents, assuming that they are of similar size. The parameter Φ is expected to be approximately constant for nitroxides exposed to the aqueous medium but to increase rapidly upon entering a hydrophobic region due to the higher membrane solubility of R_{np} compared to R_p.

In previous experiments to determine the topography of spin-labeled sites on bacteriorhodopsin using this approach, O_2 and NiAA were used as nonpolar and polar reagents, respectively. Within the bilayer interior, Φ was shown to be position dependent due to gradients of O_2 and NiAA along the bilayer normal, providing a basis for the determination of depth of immersion of a nitroxide in the bilayer (Altenbach et al., 1994).

In the present work, Φ is employed to locate the position at which the rhodopsin polypeptide enters the hydrophobic interior of the DM micelle. However, we have chosen to use NiEDDA as a polar reagent, since it is less soluble than NiAA in nonpolar regions and gives a better contrast between the two domains. This may be important in micellar systems where the transition from aqueous phase to nonpolar interior is expected to be more diffuse than in a bilayer. The function Φ was defined in terms of the *logarithm* of the ratio of $\Delta P_{1/2}$ values since the ratio spans a large numerical range throughout the bilayer thickness (Altenbach et al., 1994). In the present application there are smaller differences in $\Delta P_{1/2}(O_2)/\Delta P_{1/2}$(NiEDDA) between members of the sequence since they are all near the interface, and it is more convenient to employ the simple ratio, that is, e^{Φ}.

To calibrate the Φ parameter for O_2 and NiEDDA in DM micelles, the nitroxide containing phospholipids II(n) and III were incorporated into micelles at a total concentration of 2% DM (w/v), and the value of Φ was determined for O_2 in equilibrium with air and 20 mM NiEDDA. This concentration of DM is similar to that in the rhodopsin containing samples. Table 1 gives values of e^{Φ} for II(n) and III in DM micelles. It is evident that e^{Φ} changes abruptly in going from the head-group region in III to the micelle interior at II(5), and then gradually increases with increasing depth in the interior. Thus e^{Φ} provides sufficient contrast to distinguish water-exposed sites from micelle interior sites.

Table 1: e^{Φ} Parameter for Spin Labeled Lipids in DM Micelles[a]

lipid	e^{Φ}
III	1
II(5)	4.5
II(7)	4.8
II(10)	6.8
II(12)	7.5

[a] The DM concentration was 2% (w/v), and the molar ratio of DM to spin-labeled lipid was 1500.

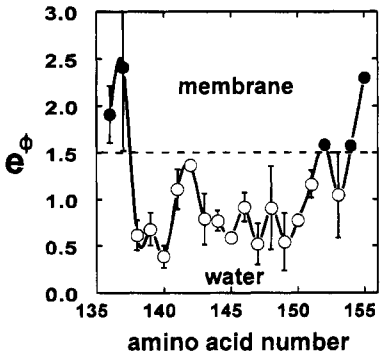

FIGURE 6: Function e^{Φ} versus amino acid position. The error bars are derived from two or more independent determinations. The relatively steep changes near the ends of the labeled sequence signify changes in the polarity of the environment, the larger values representing a decrease in polarity.

Figure 6 shows e^{Φ} values versus amino acid number through the nitroxide scan 136−155 for rhodopsin in the dark. The error bars are determined from two or more independent experiments using different batches of mutants. The errors are relatively large at some sites, possibly due to variations in the concentration of DM in the different samples and to pipeting errors in the necessarily small volumes of NiEDDA stock solutions added to the sample. Nevertheless, it is clear that e^{Φ} values for residues 138 to about 151 lie in the range of 0.4−1.4, indicating solvent exposed sites (compare with Table 1). In moving from 138 to 136, e^{Φ} increases rather steeply, suggesting a transition to a more hydrophobic environment. Similarly, at the other end of the sequence, e^{Φ} generally increases from 151 to 155, again suggesting a transition to a more hydrophobic environment. Thus the regions in the sequence at which the polypeptide chain enters a hydrophobic environment in the micelle lie between 137 and 138 and between 151−154, consistent with the model shown in Figure 1 based on hydropathy considerations. Within experimental error, no differences in Φ are found after photobleaching.

Spectral Changes Induced by Photoactivation. Figure 4A shows the first-derivative absorption spectra recorded after photoexcitation of the rhodopsin population (thin-line trace). To more clearly reveal the changes observed, the EPR difference spectra (light-dark) are shown in Figure 4B. Difference spectral amplitudes above the noise are evident for Y136R1, V138R1, V139R1, C140R1, K141R1, R147R1, G149R1, A153R1, and I154R1. The difference spectrum for K141R1 consists of a particularly sharp in-phase derivative signal. Since this is not accompanied by any significant changes elsewhere in the spectrum, it does not represent a change in mobility state of the spin population as a whole. This is confirmed by examination of the light and dark first-derivative absorption spectra. It apparently arises from the appearance of a very small population of mobile spin. The spectral change for C140R1 in DM has been previously reported (Resek et al., 1993) and was similar to that in Figure 4. The changes fall into two categories, one representing an *increase* in motional freedom, and the other a *decrease* in motional freedom upon photobleaching.[2] In the first category are Y136R1, V138R1, V139R1, and C140R1. The increase in motional freedom is revealed in the difference spectra by negative and positive signals in the region of the low and high field hyperfine extrema, respectively (arrows). For V138R1, the changes are small, but an increase in mobility is reflected by the in-phase central derivative signal in the difference spectrum.

Two sites, A153R1 and I154R1, show decreases in motional freedom, indicated by the small but definite increase in intensity of the low field hyperfine extrema. The largest light-dependent changes are detected by nitroxides in the interhelical region at R147R1 and G149R1. The nitroxides at these positions show reductions in motional freedom, distinguished in the difference spectra by the out-of-phase central derivative signal and the positive signal in the region of the resolved low field hyperine extremum.

DISCUSSION

In the preceding paper, the reactivity of single cysteine mutants in the rhodopsin sequence 136−150 were investigated (Ridge et al., 1995a). The reactivity was found to be a function of reagent, environment polarity, cysteine pK_a, and local steric constraints. In this paper, the electron paramagnetic resonance properties of nitroxide spin labels attached to single cysteine mutants in the extended rhodopsin sequence 136−155 were investigated to provide direct information on the local environment and tertiary interactions at those sites. The results provide new information on both the structure and light-dependent conformational changes in rhodopsin.

Topography of the Sequence 136−155. The topography of the rhodopsin polypeptide segment 136−155 was deduced from the variation of Φ with amino acid position. This use of Φ is based on the assumption that position-dependent steric factors that effect the collision rates of nonpolar and polar reagents with the nitroxide are similar. In this circumstance Φ reflects the ratio of local concentrations of the reagents, a quantity that is a sensitive function of solvent polarity. For O_2 and the small complex NiEDDA, the assumption of similar steric effects is reasonable for relatively mobile nitroxides on the outer surface of the protein (Altenbach et al., 1994). However, for highly constrained nitroxides with immobilized line shapes, the smaller O_2 molecules will experience less steric interference in collision than NiEDDA. As a result, Φ will be larger than expected on the basis of pure polarity considerations. This applies to Y136R1, V138R1, V139R1, C140R1, and A153R1, but uncertainties in Φ at these sites would not change the conclusions regarding the location of the micelle/solution interfaces. For example, consider the large decrease in Φ between 137 and 138. Since 137 is a mobile site, it is unaffected by this source of error. Any correction for steric effects at 138 would further *decrease* the value, enhancing the change. The increase in Φ that begins at around 151 is

[2] The term motional freedom is used in a general sense, and a change in motional freedom can arise from a change in either rate or amplitude of motion, or both.

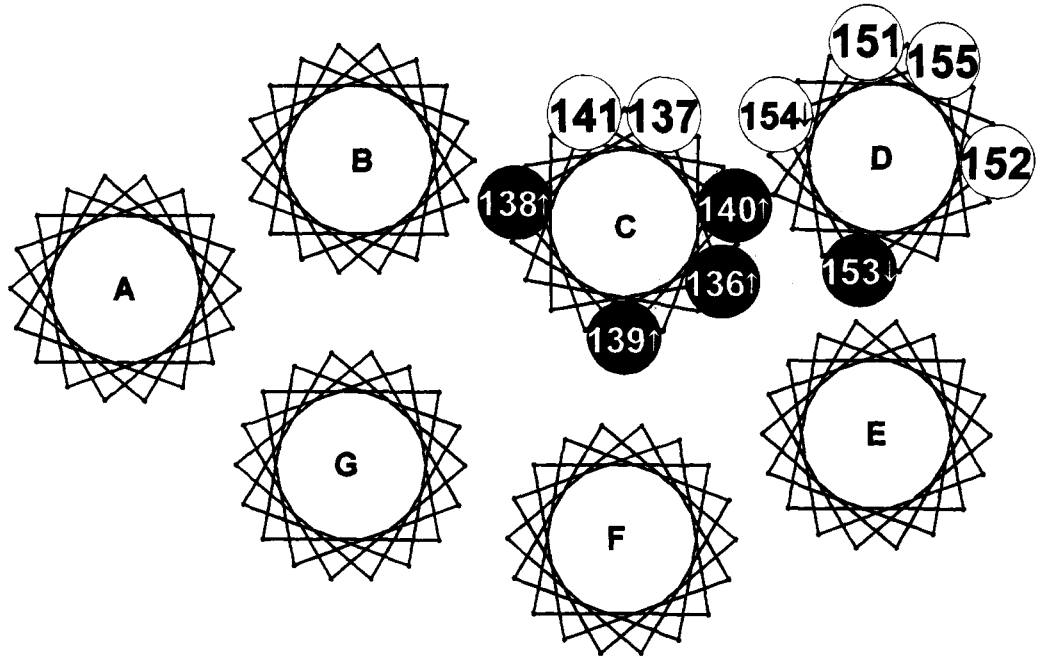

FIGURE 7: Proposed helix packing model for rhodopsin near the cytoplasmic surface [after Baldwin (1993)]. Key residues investigated in this study are noted as numbered circles. The filled and unfilled circles indicate sites with immobilized and mobile nitroxides, respectively. The arrows mark sites with decreasing motional constraints (↓) and increasing motional constraints (↑) after photoexcitation.

also not materially influenced by this error, since all but one of the side chains in this region are relatively mobile. Thus it is reasonable to assign the intersections of the nonpolar/aqueous interface with the polypeptide to be between 137 and 138 and between 151 and 154.

Another consideration in the topographical analysis is that rhodopsin is in micelles of DM rather than a membrane. Rhodopsin in solutions of this detergent has important similarities to the protein in native membranes. For example, it has high thermal stability and is regenerable with 11-*cis*-retinal after photobleaching (Knudsen & Hubbell, 1978; Sakamoto & Khorana, 1995) and activates transducin following photoexcitation (Franke et al., 1992). We assume that the hydrophobic surfaces of the protein that are solvated by the native lipid bilayer are similarly covered by the nonpolar alkyl chains of the detergent micelle. However, the micelle interfacial region is likely to be more diffuse than that for a bilayer, and in principle the location of the interface relative to the protein could be somewhat different than for a bilayer. Nevertheless, the locations of the interfaces deduced from collisional analysis are remarkably consistent with those deduced from hydropathy considerations (Figure 1).

Interpretation of the EPR Spectra in Terms of Rhodopsin Structure. The first-derivative absorption EPR spectra in the dark (Figure 4A, heavy trace) can be interpreted in terms of structure on the basis of previous work on the bacteriorhodopsin molecule, where a structural model has been derived based on electron diffraction data (Henderson et al., 1990). An important generalization from that work is that nitroxide side chains on the surface of an α-helix have a high mobility (Altenbach et al., 1993; Hubbell & Altenbach, 1994). This implies that steric restrictions due to neighboring side chains within a helix are not strong. On the other hand, *tertiary* interactions of a nitroxide side chain with other structural elements within the protein give rise to EPR spectral components that indicate significant motional constraints. This can arise either from a reduced motional rate, reduced amplitude of motion, or both (Ge & Freed, 1993). Based on these observations, some qualitative conclusions can be drawn regarding the rhodopsin structure. For example, the spectra of Y136R1, V138R1, V139R1, C140R1, and A153R1 are clearly dominated by a component in the slow motional regime, as judged by the well-defined outer hyperfine extrema (Figure 4A, arrows). These residues thus mark sites of tertiary interaction between secondary structures, such as between two α-helices.

Recently, Baldwin (1993) has proposed a model for the packing of the rhodopsin α-helices based on sequence analysis of members of the G-protein-coupled receptor family. On the basis of the location of highly conserved residues and residue polarity, it was possible to identify putative surfaces of tertiary interaction (contact surfaces of the helices) that can be compared with those identified from the spin-labeling results given above. Figure 7 shows the proposed helix packing in a plane located near the cytoplasmic region of the protein. This arrangement is consistent with the projected electron densities in rhodopsin at 9 Å resolution (Schertler et al., 1993). Baldwin terminated the helices at the proposed membrane/solution interface, but in Figure 7 the helix C is extended by ≈1 turn (see below). A distinctive feature of this model is that helix C is largely surrounded by other helices and has little contact with the lipid bilayer compared to the other helices. The filled circles in Figure 7 indicate the sites of tertiary contact identified by the spin labels and are clearly coincident with those predicted by the model if the helices are extended above the membrane/solution interface to the extent mentioned above.

A further comparison can be made between the model and other labeled sites. For example, the model predicts that V137R1, K141R1, N151R1, H152R1, I154R1, and M155R1 should all be at noninteracting surfaces of the α-helices as indicated in Figure 7 (open circles) and should therefore have spectra characteristic of more mobile R1 side chains.

Examination of the spectra in Figure 4 shows that this is qualtitatively the case.

Residues K141R1−H152R1 are all in contact with the aqueous medium (Figure 6) and comprise the C−D interhelical region. The spectra are complex with line shapes suggestive of multiple states of the side chains. There is no obvious periodic variation in spectral properties, and no conclusion can be reached regarding possible secondary structure in this region.

Light-Dependent Structural Changes. In earlier work, EPR spectral changes induced by light were detected at C140R1 near the termination of the C helix (Resek et al., 1993; Farahbakhsh et al., 1993), and the present experiments explored the region around this site in more detail. The light-dependent changes in the sequence 136−155 are not global: of the 20 sites examined, only eight show detectable changes in motional constraints upon photoexcitation (Figure 4). Six of these are identified by arrows in Figure 7. It is significant that all four of the sites defining the putative tertiary contact surface of helix C are involved (Y136R1, V138R1, V139R1, and C140R1). Since the spectral changes represent *decreases* in motional restriction, a simple interpretation is an outward movement of helix C relative to B, D, E, F, and G. The lack of spectral change for nitroxides on the exposed surface of the C (K141R1, V137R1) and D (N151R1, H152R1, I154R1, M155R1) helices implies that no alteration in secondary structure accompanies the modulation of tertiary contact discussed above. This is consistent with a rigid-body motion of helix C.

In the context of the above model and assuming rigid body helix movements, the helix movement would have to be smaller than about 5 Å, the approximate length of the side chains, since a larger motion would disengage the interacting surfaces to an extent that would allow much greater freedom of motion of the nitroxide than is observed after bleaching. The spectral changes at A153R1 and I154R1 are very small but suggest an increase in motional restriction at these sites. The change at I154R1 could be accounted for by an outward movement of helix C which would increase tertiary interaction at that site, but the change at 153 would appear to require a movement of helix D and/or E.

The large light-induced spectral changes for R147R1 and G149R1 demonstrate perturbations in the C−D interhelical loop or neighboring structures. No experimental information is available regarding the conformation of this region, and it is not possible to speculate on the nature of the structural changes. However, this interhelical region has been shown to be involved in transducin activation, and it is significant that mutations at positions R147R1 and G149R1 have the largest effect on the yield of chromophore formation of any of the residues in the C−D interhelical loop (Ridge et al., 1995a). Finally, the fact that Φ does not change significantly upon bleaching suggests that helices C and D do not undergo vertical displacements relative to the other helices (Altenbach et al., 1994).

Do these changes represent a biochemically significant event? In earlier work, a change at C140R1 was observed for rhodopsin in the native disk membranes upon photoexcitation (Farahbakhsh et al., 1993). Although the nature of the spectral change was different than for rhodopsin in DM micelles, this result suggests that the light-induced change in structure at this site does not require a micellar environment (Resek et al., 1993). The EPR spectral changes in the disk membrane were time-resolved and found to have the same kinetics and activation energy as the appearance of MII, the active form of the receptor. Furthermore, the spectral change at C140R1 in DM micelles was shown to be absent in digitonin micelles, where the protein is arrested at the MI stage (Resek et al., 1993). These results suggest that the changes observed here for the C helix sites in the vicinity of C140 are relevant to receptor activation and related to the formation of MII. We note, however, that the light-induced change detected by a spin label at C316R1 near the termination of helix G was considerably larger for rhodopsin in DM micelles than in the native membrane (Resek et al., 1993; Farahbakhsh et al., 1993). Thus the magnitude of the structural change is apparently modulated by the environment of the protein, a conclusion in harmony with earlier experiments that demonstrated conformational changes of the protein dependent on the chain length of the phospholipids in reconstituted membranes (Farahbakhsh et al., 1992). Finally, it is clear that the changes observed in DM micelles do not represent a global unfolding of the protein, since they are rather localized (Figure 4).

An entirely different line of evidence points to a possible functional role for the movement of helix C. In the ground state protein, 11-*cis*-retinal forms a protonated Schiff base with K296 on helix G. The counterion is provided for by E113 on helix C (Sakmar et al., 1989; Zhukovsky & Oprian, 1989; Nathans, 1990). This salt bridge is in a low dielectric environment and could be quite strong (Honig & Hubbell, 1984). Mutagenesis results from Oprian and colleagues suggest that this salt bridge stabilizes the inactive ground state of rhodopsin (Robinson et al., 1992; Cohen et al., 1993). Upon photoactivation, the Schiff base is deprotonated at MII, the active state. The loss of both the salt bridge and the interaction with the 11-*cis*-retinal chromophore removes important structural constraints on the protein, and this situation may allow the thermal motion of helix C relative to G.

REFERENCES

Altenbach, C., Flitsch, S. L., Khorana, H. G., & Hubbell, W. L. (1989) *Biochemistry 28*, 7806−7812.

Altenbach, C., Marti, T., Khorana, H. G., & Hubbell, W. L. (1990) *Science 248*, 1088−1092.

Altenbach, C., Greenhalgh, D. A., Khorana, H. G., & Hubbell, W. L. (1993) *Biophys. J. 64*, A51.

Altenbach, C., Greenhalgh, D. A., Khorana, H. G., & Hubbell, W. L. (1994) *Proc. Natl. Acad. Sci. U.S.A. 91*, 1667−1671.

Baldwin, J. M. (1993) *EMBO J. 12*, 1693−1703.

Cohen, G. B., Yang, T., Robinson, P. R., & Oprian, D. D. (1993) *Biochemistry 32*, 6111−6115.

Chothia, C., & Lesk, A. M. (1985) *J. Mol. Biol. 115*, 116−118.

Farahbakhsh, Z. T., Altenbach, C., & Hubbell, W. L. (1992) *Photochem. Photobiol. 56*, 1019−1033.

Farahbakhsh Z. T., Hideg, K., & Hubbell W. L. (1993) *Science 262*, 1416−1419.

Franke, R. R., Sakmar, T. P., Graham, R. M., & Khorana, H. G. (1992) *J. Biol. Chem. 267*, 14767−14774.

Ge, M., & Freed, J. H. (1993) *Biophys. J. 65*, 2106−2123.

Greenhalgh, D. A., Altenbach, C, Hubbell, W. L., & Khorana, H. G. (1991) *Biochemistry 88*, 8626−8630.

Henderson, R., Baldwin J. M., Ceska, T. A., Zemlin, F., Beckmann, E., & Downing, K. H. (1990) *J. Mol. Biol. 213*, 899−929.

Honig, B. H., & Hubbell, W. L. (1984) *Proc. Natl. Acad. Sci. U.S.A. 81*, 5412−5416.

Hubbell, W. L., Froncisz, W., & Hyde, J. S. (1987) *Rev. Sci. Instrum. 58*, 1879−1886.

Hubbell, W. L., & Altenbach, C. (1994) *Curr. Opin. Struct. Biol. 4*, 566−573.
Karnik, S. S., Sakmar, T. P., Chen, H.-B., & Khorana, H. G. (1988) *Proc. Natl. Acad. Sci. U.S.A. 85*, 8459−8463.
Karnik, S. S., Ridge, K. D., Bhattacharya, S., & Khorana, H. G. (1993) *Proc. Natl. Acad. Sci. U.S.A. 90*, 40−44.
Khorana, H. G. (1992) *J. Biol. Chem. 267*, 1−4.
Knudsen, P., & Hubbell, W. L. (1978) *Membr. Biochem. 1*, 297−322.
Konig, B., Arendt, A., McDowell, J. H., Kahlert, M., Hargrave, R. A., & Hofmann, K. P. (1989) *Proc Natl. Acad. Sci. U.S.A. 86*, 6878−6882.
McPhalen, C. A., Vincent, M. G., Picot, D., Jansonius, J. N., Lesk, A. M., & Chothia, C. (1992) *J. Mol. Biol. 227*, 197−213.
Nathans, J. (1990) *Biochemistry 29*, 9746−9752.
Oprian, D. D., Molday, R. S., Kaufman, R. J., & Khorana, H. G. (1987) *Proc. Natl. Acad. Sci. U.S.A. 84*, 8874−8878.
Ovchinnikov, Y. A. (1982) *FEBS Letters 148*, 179−190.
Resek, J., Farahbakhsh, Z. T., Hubbell, W. L., & Khorana, H. G. (1993) *Biochemistry 32*, 12025−12032.
Ridge, K. D., Zhang, C., & Khorana, H. G. (1995a) *Biochemistry 34*, 8804−8811.
Ridge, K. D., Lu, Z., Liu, X., & Khorana, H. G. (1995b) *Biochemistry 34*, 3261−3267.
Robinson, P. R., Cohen, G. B., Zhukovsky, E. A., & Oprian, D. D. (1992) *Neuron 9*, 719−725.
Sakamoto, T., & Khorana, H. G. (1995) *Proc. Natl. Acad. Sci. U.S.A. 92*, 249−253.
Sakmar, T. P., Franke, R. R., & Khorana, H. G. (1989) *Proc. Natl. Acad. Sci. U.S.A. 88*, 3079−3083.
Schertler, G. F. X., Villa, C., & Henderson, R. (1993) *Nature 362*, 770−772.
Shin, Y. K., Levinthal, F., Levinthal, C., & Hubbell, W. L. (1993) *Science 259*, 960−963.
Steinhoff, H. J., Mollaaghababa. R. Altenbach, C., Hideg, K., Krebs, M., Khorana, H. G., & Hubbell, W. L. (1994) *Science 266*, 105−107.
Zhukovsky, E. A., & Oprian, D. D. (1989) *Science 246*, 928−930.

BI950364H